POSSIBLE USE OF HIGH RESOLUTION BSPM DATA FOR MODEL-BASED METHODS FOR HEART STATE ASSESSMENT

M Tysler*, M Turzova*, M Tinova*,V Szathmary**, S Filipova***

*Institute of Measurement Science and **Institute of Normal and Pathological Physiology, Slovak Academy of Sciences, Bratislava, Slovakia
***Department of Cardiology, Institute of Cardiovascular Diseases, Bratislava, Slovakia

Abstract
Results of a simulation study and experimental verification of a non-invasive assessment of the heart state using high resolution body surface potential mapping in two different pathological conditions are presented in the paper. A computer model was used to simulate normal and changed depolarization and repolarization of the myocardium and to compute potential distribution on the surface of a realistic inhomogeneous torso.
Single accessory pathway in WPW syndrome was simulated in different positions along the atrio-ventricular ring. Noninvasive localization of the arrhythmogenic tissue was based on a restricted single or multiple dipole model of the cardiac generator. If 63 leads were used, noise was less than 5 μV and heart position error in inhomogeneous torso was less than 10 mm, positions of the accessory pathway could be obtained with a mean localization error of 11 -17 mm. Method based on single dipole was more robust than the multiple dipole model. Experimental noninvasive localization of the accessory pathway in a WPW patient was in good agreement with the invasively obtained site.
Local repolarization changes were simulated in subendocardial and transmural regions comprising 3-12% of the ventricular volume and situated in antero-septal or postero-lateral part of the left ventricle. Changed repolarization was clearly reflected in QRST integral maps. The changes in maps were significantly smaller if the regions were transmural. Difference integral maps and a dipole model based method could be used for successful non-invasive localization of the heart segment with changed repolarization in small subendocardial regions.

1. Introduction

Some types of cardiac arrhythmias have their origin in small localized areas of the myocardium. This is also the case of Wolff-Parkinson-White (WPW) syndrome, where an abnormal conducting tissue (accessory pathway) exists at the atrio-ventricular ring. The most precise localization of the substrate has been provided invasively during catheterization from electrograms measured directly on the heart during radio-frequency catheter ablation. However, non-invasive prediction of the location of the substrate can substantially shorten and simplify the invasive procedure. A simulation study and an experimental verification of the possibility to find single accessory pathway by a non-invasive model-based approach using body surface potential maps and information on patient torso geometry is presented in this paper.
Ventricular repolarization expressed in the ST-T part of the ECG signals is closely related to the shape of action potentials (AP) of myocardial cells. Variations of AP shapes in different myocardial layers and distribution of action potential duration (APD) through the ventricular walls are substantial for resultant repolarization process. In the study, realistic AP shapes were used to simulate normal heart repolarization as well as repolarization with locally changed APD in areas of various sizes and in different heart regions. Corresponding surface ECG potentials were computed and used to investigate the ability of body surface potential

mapping methods to detect and localize such repolarization changes that are characteristic for ischemic tissue.

2. Method and material

High resolution body surface potential maps (BSPM) and models of the cardiac electric generator were used to assess the heart state in two pathological conditions: in WPW syndrome with single accessory pathway and during local ischemic changes in the left ventricle.

Sites of the abnormal activation in WPW syndrome were localized by inverse computations from BSPM during the initial phase of the ventricular depolarization and using geometry of the patient torso. Restricted single dipole or multiple dipole was used as the model of the cardiac electric generator and their position identified the site of the accessory pathway.

Locations of small repolarization changes caused by local ischemia in different heart regions were assessed using the differences between normal and changed BSPM. These differences were interpreted as being caused by an additional dipole source corresponding to the changed AP during the repolarization phase and were localized by a restricted single dipole model. To increase sensitivity of the method, integral maps over a time interval containing the whole repolarization period were used in the study. Relative RMS differences D were evaluated to estimate the possibility to detect the changes in measured maps:

$$D = \frac{\sqrt{\frac{1}{N}\sum_{i=1,N}(S_i - A_i)^2}}{\sqrt{\frac{1}{N}\sum_{i=1,N}A_i^2}}$$

where Si are values in changed integral map,
Ai are values in normal integral map,
N is number of mapped points.

:

Both methods were tested on simulated surface potentials. Several error factors influencing accuracy of the inverse procedure were analyzed to estimate their performance. Localization of the accessory pathway in WPW was verified on a measured patient data.

A forward model was used to get well defined simulated body surface potentials in a normal case as well as in the two pathological cases. In the first one, WPW syndrome with single accessory pathway was simulated by abnormal depolarization of the ventricles that started in predefined positions along the atrio-ventricular ring. In the second one, local ischemia was simulated by areas with changed APD that were defined in different regions of the left ventricle.

2.1. Models of cardiac generator used for assessment of the heart state

Two types of equivalent cardiac generator based on current dipole source were considered to find the position of the accessory pathway or region with changed repolarization:

Restricted single dipole (JD). In JD model, the myocardium was divided into 28 or 39 segments (Fig. 1) and cardiac generator was modeled by single segmental dipole successively. for each segment *i=1,2,...n.* The best dipole estimation was obtained using the formula:

$$\boldsymbol{D_i(t) = T_i^{+}\,\Phi(t)}$$

where $\Phi(t)$ are body surface potentials,
$\boldsymbol{T_i^{+}}$ is pseudoinverse of the transfer matrix
$\boldsymbol{D_i(t)}$ are components of i-th segmental dipole

Transfer matrix $\boldsymbol{T}$ represents the relation between positions of the dipoles and the surface potentials. Pseudo-inverse $\boldsymbol{T}^{+}$ was obtained by truncated singular value decomposition and used to solve the ill posed inverse problem.

For all segmental dipoles estimated in this way, surface ECGs were computed and compared

to original potentials. Minimal RMS difference between original and computed potentials during the evaluated time interval indicated most probable segment with the equivalent dipole source causing the initial ventricular activation or changed repolarization of ventricles. To improve stability of the solution in the WPW case, minimum of the sum of relative RMS errors during the initial interval of activation (from 7.5 to 25 ms) was used.

Multiple Dipole (MD). The MD model composed of a number of segmental dipoles was alternatively used for identification of the segment with accessory pathway. Heart ventricles were partitioned into 39 segments and segmental dipoles were located at the centers of these segments. Orthogonal components of segmental dipoles ***M*** in time ***t*** were estimated using the formula:

$$\boldsymbol{M(t) = T^{+}\,\Phi(t)}$$

where $\boldsymbol{\Phi(t)}$ are body surface potentials,
$\boldsymbol{T^{+}}$ is pseudoinverse of the transfer matrix
$\boldsymbol{M(t)}$ are components of segmental dipoles

As a criterion for identification of the segment with initial activation, maximal magnitude of a dipole moment was used. Segmental dipoles were computed for several time instants during the initial interval of activation. Summation of dipole moments over the initial interval of activation (first 20-25 ms) was used to stabilize the inversely determined segment.

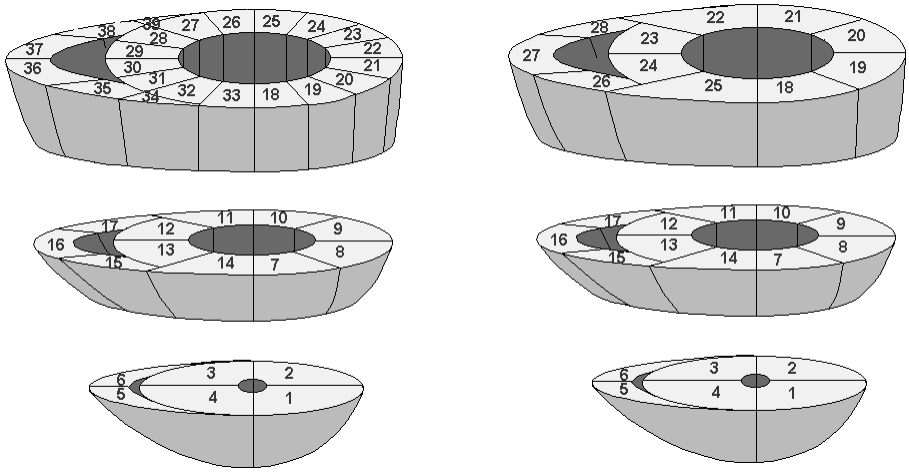

Fig. 1. Segmentation of ventricles to 39 segments (16 are on the atrio-ventricular ring) for accessory pathway localization and to 28 segments for identification of local ischemia.

2.2. Simulation of normal and abnormal heart activation

To simulate the surface potentials, a forward model with three basic components was used: (1) finite element model of the heart ventricles, (2) equivalent multiple dipole model of the generator and (3) boundary element method for potential computation in piecewise homogeneous torso.

Finite element model of heart ventricles with analytically defined geometry shown in Fig. 2 and with element size of about 1 mm^3 [1] was used to simulate the ventricular depolarization and repolarization. Normal depolarization was started at points of early activation that were experimentally observed in normal human hearts. Spread of activation in isotropic myocardial tissue was governed by cellular automaton. A layer with three times increased conduction velocity was used at the endocardial surface to simulate the Purkinje fibers.

Linear AP shape was used to simulate the initial ventricular depolarization in WPW. Different AP shapes in up to five layers from epicardium to endocardium were defined in ventricular walls and in the septum to simulate the repolarization (Fig.3). Realistic AP shapes measured in canine left ventricular wedge preparation [2] were adopted in this study. Experimentally

observed distribution of APD [2, 3] was preserved in the simulations and their transmural dispersion was about 40 ms with shorter APD at the epicardial surface.

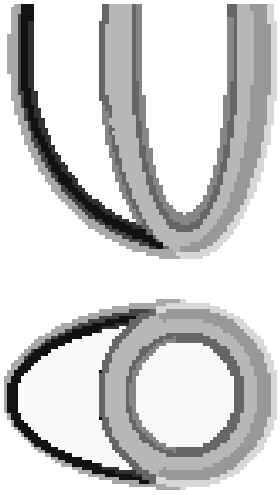

Fig. 2. Analytically defined ventricular volume composed of ellipsoids.

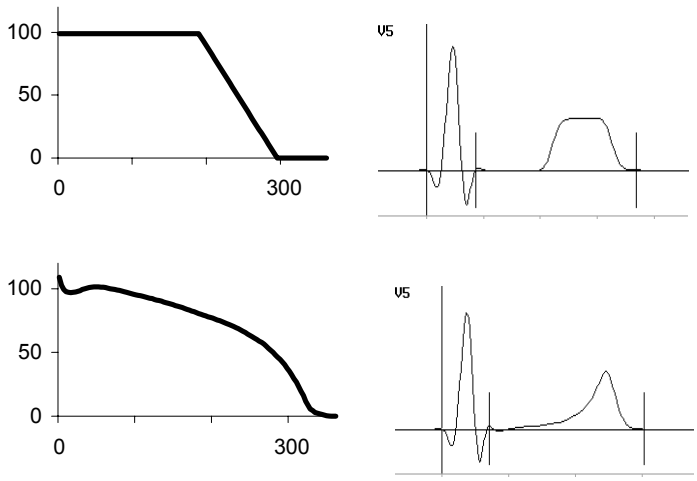

Fig. 3. Linear and realistic form of the action potential used in the study and their influence on the simulated surface ECG.

Besides normal activation, also depolarization in WPW syndrome and repolarization influenced by local ischemia were simulated.
To simulate different cases of WPW syndrome with single accessory pathway, ventricular depolarization was initiated in 8 physiologically defined regions on the epicardial surface along the atrio-ventricular ring [4] (Fig. 4).

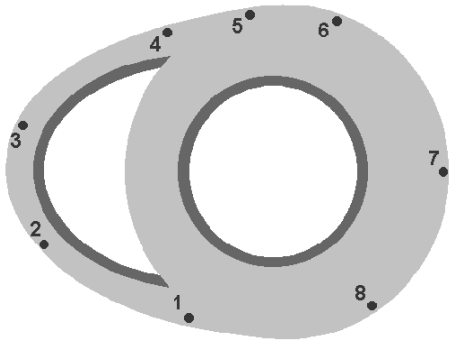

Fig. 4. Simulated positions of single accessory pathway along the atrio-ventricular ring: 1.anterior septal, 2. anterior RV, 3. lateral RV, 4. posterior RV, 5. posterior septal, 6. posterior LV, 7.lateral LV, 8. anterior LV

Changed repolarization of ventricles during ischemia was simulated by APD locally changed by -5 % to -20 % from the normal values. Two regions of changed AP with lesions of three different sizes were defined in the LV as shown in Fig.5: antero-septal near the apex (A1 is 3%, A2 is 6% and A3 is 10% of the ventricular volume) and postero-lateral close to the heart base (P1 is 4%, P2 is 8% and P3 is 12% of the ventricular volume). Small and medium regions were subendocardial while the large regions A3 and P3 were transmural.

Fig. 5. Heart regions with changed repolarization in the LV.
Left: antero-septal regions. Right: postero-lateral regions.
Cuts are through the lesion centers, larger lesions are darker.

To make the computation of surface potentials easier, multiple dipole model having 168 dipoles was used to represent the cardiac electric generator. Each of the dipoles was obtained as a sum of elementary dipoles in one of 168 anatomically defined heart segments.
Boundary element method was employed to compute potentials on the surface of a realistic inhomogeneous torso model comprising lungs and heart ventricles with conductivities equal to 0.25 and 3.0 times the torso conductivity, respectively (Fig. 6).

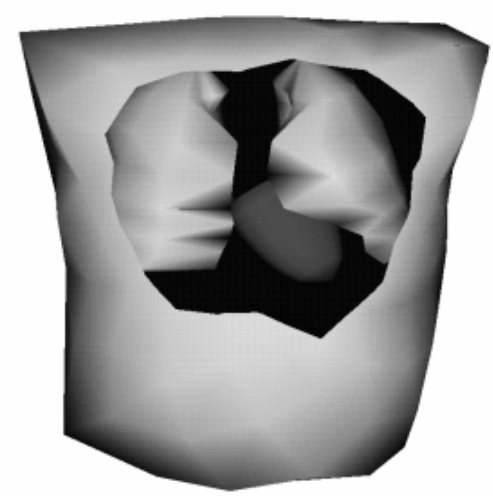

Fig. 6. Realistic inhomogeneous torso model with heart and lungs was used in the study.

2.3. Simulation of error factors

Influence of some factors causing error in the localization of the accessory pathway was analyzed for both models. Incomplete knowledge of the thorax geometry was represented by neglecting of lungs and heart cavities. Errors in determination of the heart position were simulated by shifts and rotations of the equivalent generator (misplacements of initial sites of activation were about 1 cm). Noise with normal distribution and standard deviation 3 - 20 μV was added to simulated surface potentials. Accuracy of inverse computations from potentials simulated in 198 points defining the whole surface of the model torso and in several practically used mapping lead sets with 24 to 63 unipolar electrodes was estimated by mean localization error (MLE). MLE greater than 3 cm was considered as a localization failure.

2.4. Verification on real data

For one WPW patient complete data measured by Shadidi et al. [5] were used. ECG potentials in 63 mapping leads and the shape of thorax with lungs and ventricles including cavities (based on CT scans) were available and used in the inverse computations. Intraoperative measurements of epicardial potentials localized the preexcitation site at the base of the lateral wall of the left ventricle.

To test the influence of incomplete geometry knowledge on the inverse computations, real chest with analytically approximated heart geometry and some standard chest and heart geometry were used besides the real patient chest geometry (Fig. 7) [6].

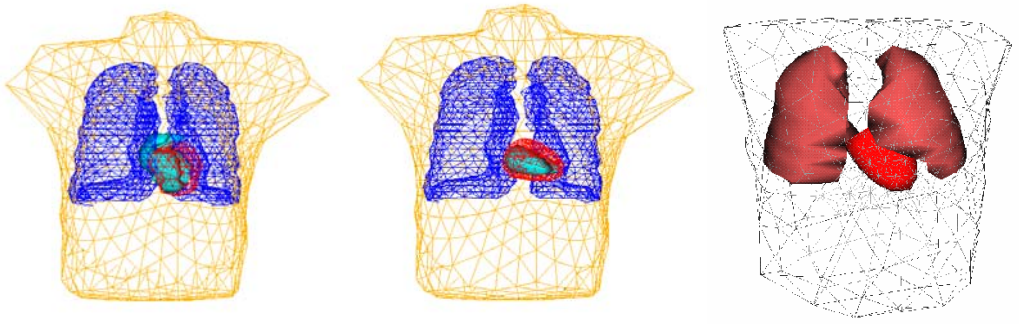

a) **b)** **c)**

Fig. 7. Torso geometry used for accessory pathway localization in the WPW patient: a) real individual geometry, b) analytical approximation of the heart in real chest with lungs, c) standard chest model with analytically approximated heart .

3. Results

3.1 Assessment of accessory pathway in WPW syndrome

MLE of the accessory pathway localization from simulated BSPM using different ECG lead sets are shown in Table 1. When no noise and error factors were present, 32 or more leads enabled acceptable localization of the accessory pathway.

The influence of heart misplacement was similar for both methods. On the other hand, the influence of torso inhomogeneities and especially noise in BSPM was higher in the MD-based method. In Fig. 8, sensitivity of the JD- and MD-based methods to the noise and to decreasing number of measured leads is demonstrated for BSPM measured in 198 points over the whole torso and in 63 mapping leads. For noise less than 5 μV, the performance of both methods was similar, however, when the noise rose, the MLE of the MD-based method increased faster, especially for 63 leads.

Lead set Number of leads	**Mean localization error [cm]**			
	JD model		**MD model**	
	Inhomogen.	**Homogen.**	**Inhomogen.**	**Homogen.**
Torso 198	0.5	0.6	0.6	1.1
Savard 63	0.5	0.8	0.6	1.1
Lux 32a	0.4	0.5	1.5	2.1
Barr 24	0.9	1.0	*3,2	*2.4

Table 1: Influence of the lead set on the mean localization error

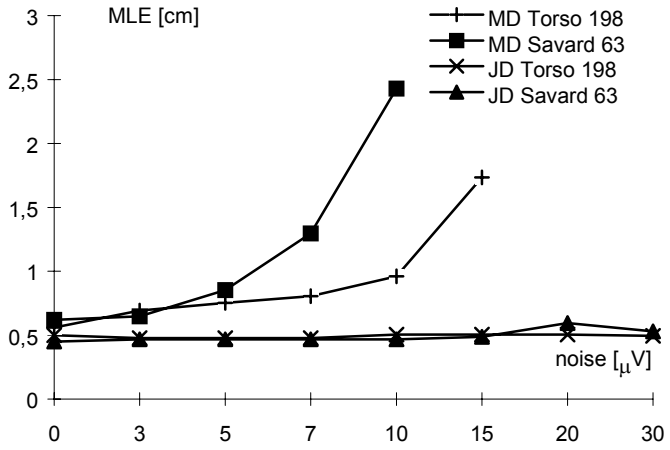

Fig 8: Influence of noise in BSP on the MLE of the accessory pathway computed from simulated potentials in 198 or 63 leads

When accessory pathway was localized from 63 leads, acceptable results were obtained with the JD-based method even if all error factors were combined (Table 2). The influence of inaccurate knowledge of heart position was similar for both models. On the other hand, influence of torso inhomogeneities and noise in ECG was higher in the MD model. No failures occurred with the JD model.

Error factors (Number of simulations)	**Mean localization error [cm]** (Failures)	
	JD model	**MD model**
no (8)	0.5	0.6
homogeneous torso (8)	0.8	1.1
noise 5 μV (40)	0.5	0.8
heart misplacements (40)	1.0	0.9
combined factors (200)	1.1	1.7 (14 %)

Table 2: Results of simulated accessory pathway localization from 63 leads influenced by different error factors.

For 63 ECG leads measured in the WPW patient, several torso geometry configurations were tested (Table 3) in the inverse computations. Both models were able to localize the accessory pathway within 1 or 2 segments if real inhomogeneous torso was used (Fig.9). With the JD model, accessory pathway site was correctly localized even if approximate heart geometry and homogeneous torso model was used.

Torso geometry	**JD model**		**MD model**	
	Inhomogeneous	**Homogeneous**	**Inhomogeneous**	**Homogeneous**
Real	19	19	20	34
Analytical	19	19	20	7
Standard	19	20	7	18

Table 3: Segments with localized accessory pathway in the patient measured in 63 ECG leads (actual site of accessory pathway was in segments 19-21, see Fig. 5)

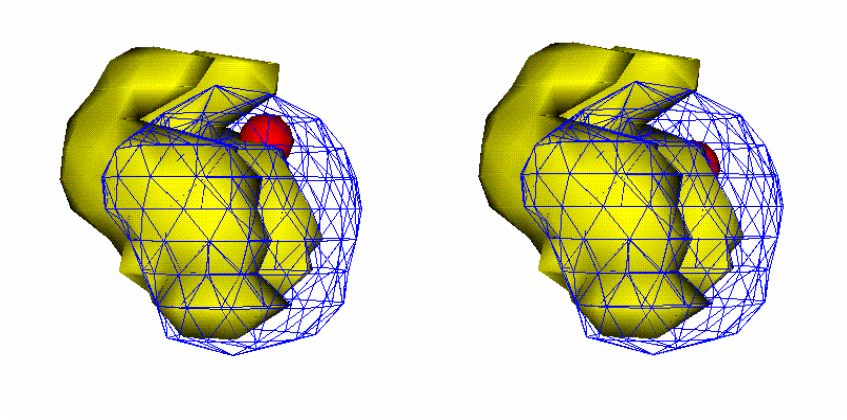

a) **b)**

Fig. 9. Site of noninvasively localized accessory pathway in a WPW patient (when real cest and heart geometry was used):
a) using JD model. (Localization corresponds to segment 19)
b) using MD model. (Localization corresponds to segment 20)

3.2 Assessment of local repolarization changes in ischemia

QRST body surface integral maps were used for identification and localization of local repolarization changes. In all simulated cases, changes in the maps were clearly visible and regions with changed AP were projected to areas of changes in integral maps that appeared in corresponding locations over the torso surface. Properly located changes in integral maps were visible also for all AP changes in postero-lateral LV regions.
In Fig. 10 is example of simulated normal QRST map and maps obtained if AP was shortened by 20% in antero-septal and postero-lateral regions of medium size (A2, P2). AP shortening is projected as decrease of the QRST integral mainly on the near-by left anterior and mid posterior torso surface, respectively.

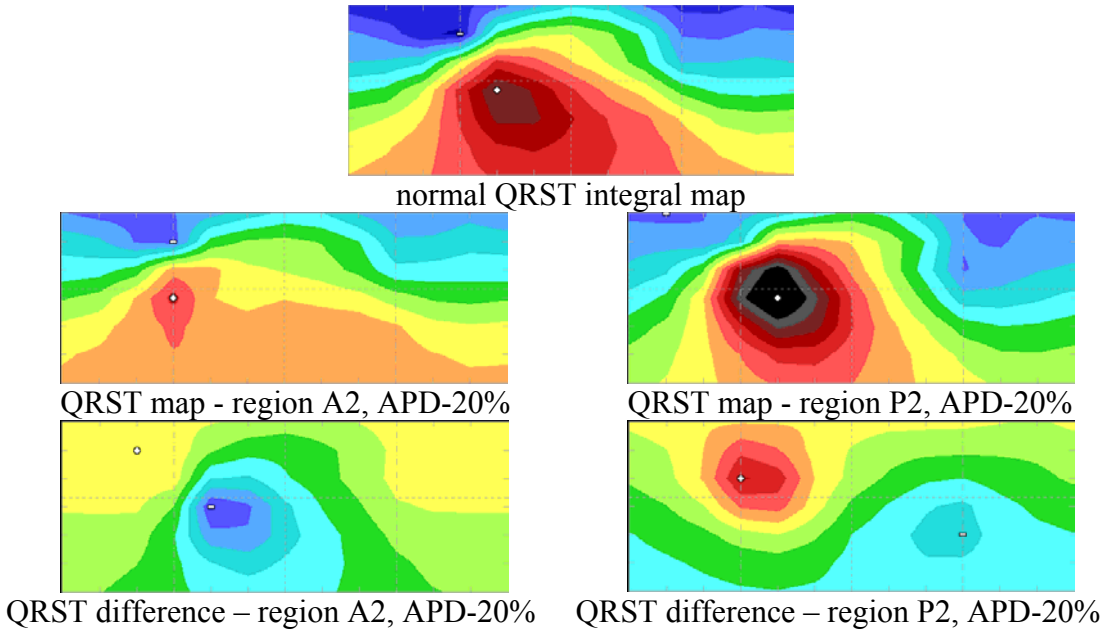

Fig. 10. QRST integral maps for simulated normal activation, QRST integral maps and difference integral maps for simulated APD shortened by 20% in antero-septal and postero-lateral lesions of medium size.

Relative RMS differences between normal and changed QRST integral maps (Fig. 11) reached values from 10% to 45% and were proportional to APD changes. However, the differences did correspond with the lesion size only for subendocardial regions while large transmural regions produced smaller differences with flatter extremes than medium subendocardial lesions. This was true for APD changes in both, antero-septal and postero-lateral regions of the LV.

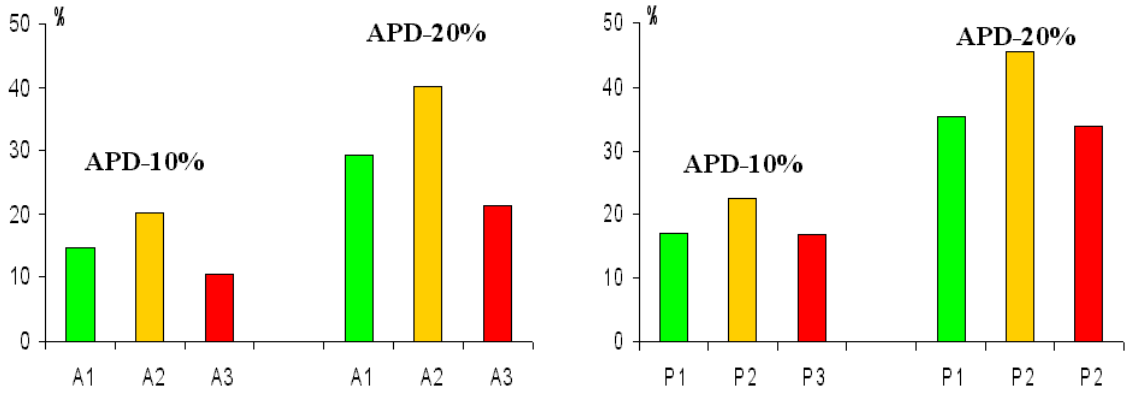

Fig. 11. Relative RMS difference between normal and changed QRST integral maps for APD shortening by 10% and 20% in lesions of all 3 sizes in both, antero-septal (left) and postero-lateral (right) regions of the LV.

Results of the inverse localization of the lesions with APD decreased by 20 % to one of 28 ventricular segments are shown in Table 4. Positions of the lesions borders and detected heart segments are in good correspondence in all cases, except the transmural lesion A3 that was detected in the mid septal segment that is too far to the right (see Fig. 1 and 5). Similar results were obtained for other APD changes.

Region and size		Segment
Antero-septal	A1	1
	A2	7
	A3	12
Postero-lateral	P1	21
	P2	21
	P3	10

Table 4. Inverse localization of lesions with APD shortening by 20% to 1 of 28 segments (see Fig.1) using single restricted dipole.

4. Discussion and conclusions

Presented simulation results suggest that high resolution BSPM data together with known patient torso geometry can be used for noninvasive assessment of the heart state in selected situations. However, when interpreting the results, some limitations of the study have to be taken into account.

Because of the limitations of the forward model, validity of the obtained results has to be thorougly verified on real data. The main limitation of the model is the simple heart geometry without atria an use of isotropic myocardium. Further, action potential shapes and durations in the myocardium elements were defined a priori and their possible mutual influence

(electrotonic coupling) was not considered. Therefore, careful adjustment of APD and other AP characteristics was necessary to obtain realistic simulated potentials. All these factors may cause inaccuracy of simulated surface potentials that should be considered when interpreting the results.

Moreover, in real situations, namely the identification of local repolarization changes can be masked by other physiological fluctuations and noise in measured data. Our attempt to detect the changes by departure integral maps showed that the ECG changes are relatively small when compared with normal inter-individual fluctuations and can hardly be detected by departure integral maps. In real measurements, difference integral maps probably have to be corrected to suppress other physiological variability (e.g. different heart rate before and after exercise test). Only detection of APD changes during repolarization was presented in the study. Simultaneous changes of AP amplitudes present in real data should not invade the basic results of the simulation because of the positive synergetic effect of both, APD shortening and amplitude decrease, on the integral maps. Use of QRST integrals in the study was based on the fact that the depolarization was not changed at all in the simulations. In reality, this might not be true and use of ST-T integrals may be more appropriate with real data.

Despite the limitations of the study, presented results indicate that both JD and MD model based methods might be able to determine the position of single accessory pathway in WPW syndrome within one of 16 regions along the atrio-ventricular ring with acceptable localization error if at least 63 ECG leads are measured, realistic torso geometry is used, noise in ECG is less than 5 μV and inaccuracy of heart position is less than 10 mm. For the MD model, mean localization error 1.7 cm and for the JD model about 1.1 cm can be expected. Generally, the JD-based method performed better and was less sensitive to noise in ECG and geometry inaccuracy than the MD-based method. Presented localization of single accessory pathway in a real patient was in good agreement with invasively obtained site. Localization from 63 measured leads using individual torso geometry was successful with both, MD and JD model based methods.

Results of the simulations also suggest that local repolarization changes in different heart regions could be observed in changed QRST integral maps. In most cases, difference between normal and changed integral maps (for example before and after exercise test or during repeated measurements over a long time period) could be used to localize a dipole sources corresponding to the small region of changed repolarization. However, transmural lesions produce less difference in the maps and their identification is more difficult. For larger lesions, single dipole model is probably not adequate and the localization may not be in correspondence with the real lesion border. In real situations, identification of the lesion may be complicated namely by noise in ECG, unknown torso geometry and changed heart rhythm.

Acknowledgements

This work was supported by grants 2/1135/23 and 2/3203/23 from the VEGA grant agency.

References

[1] Szathmáry V, Ruttkay-Nedecký I. Effects of different sources of ventricular repolarization heterogeneity on the resultant cardiac vectors. A model study. In: Gy. Surján, R. Engelbrecht, P. McNair (eds.) Health Data in the Information Society. Proceedings of MIE2002, IOS Press, Amsterdam, 2002, 88-92.

[2] Yan GX., Shimizu W, Antzelevich Ch. Characteristics and distribution of M cells in anterially perfused canine left ventricular wedge preparations. Circulation, 1998, 98: 1921-1927.

[3] Li GR, Feng J, Yue L, Carrier M. Transmural heterogeneity of action potentials and Ito1 in myocytes isolated from the human right ventricle, Am J Physiol., 1998, 275: H369 – H377.
[4] Tyšler M, Turzová M, Tiňová M, Švehlíková M. Accuracy evaluation of non-invasive localization of accessory pathways. Biomedizinische Technik, 1997, 42: Ergänzungsband 1, 281-284.
[5] Shahidi AV, Savard P, Nadeau R. IEEE Trans. Biomed. Eng., 1994, 41: 249-256.
[6] Tiňová M, Tyšler M, Turzová M. Inverse localization of preexcitation sites using a jumping dipole. Journal of Electrocardiology, 1997, 30: 348.

Address for correspondence:

Dr. Milan Tysler
Institute of Measurement Science, Slovak Academy of Sciences
Dubravska cesta 9, 841 04 Bratislava, Slovakia
E-mail address: umertysl@savba.sk